Few-Body Systems 30, 65–79 (2001)

Few-Body Systems

Proton-Induced Deuteron Breakup Reaction at 65 MeV: Unspecific Configurations*

K. Bodek[1], J. Golak[1], L. Jarczyk[1], St. Kistryn[1], J. Kuroś-Żołnierczuk[1], J. Lang[2], A. Micherdzińska[3], R. Skibiński[1], J. Smyrski[1], M. Sokołowski[1], J. Sromicki[2], A. Strzałkowski[1], H. Witała[1], J. Zejma[1], and W. Zipper[3]

[1] Institute of Physics, Uniwersytet Jagielloński, ul. Reymonta 4, PL-30059 Kraków, Poland
[2] Institute for Particle Physics, Eidgenössische Technische Hochschule, Hönggerberg, CH-8093 Zürich, Switzerland
[3] Institute of Physics, Uniwersytet Śląski, ul. Uniwersytecka 4, PL-40007 Katowice, Poland

Abstract. Cross sections and vector-analyzing powers for four unspecific configurations of the ^{2}H$(\boldsymbol{p}, pp)n$ breakup reaction at $E_p^{\rm lab} = 65$ MeV were measured in a kinematically complete experiment. Measured observables are compared with rigorous Faddeev calculations using four realistic charge-dependent interaction models, the CD Bonn, Argonne v_{18}, Nijmegen I, and Nijmegen II potentials with or without inclusion of the Tucson-Melbourne three-nucleon force. Coulomb effects are completely omitted. A satisfactory agreement between theory and experiment has been found. There exist, however, some discrepancies between measured and calculated analyzing-power distributions in certain kinematical regions. The effects of the Tucson-Melbourne three-body force are either negligible or slightly increasing the disagreement.

1 Introduction

For many years the nucleon-nucleon (NN) interaction has been one of the most intensively investigated fields in nuclear physics. The majority of modern theoretical models of the NN interaction has achieved a maturity so as to provide realistic two-nucleon ($2N$) potentials describing the existing NN data with unprecedented accuracy, typically with a χ^2/data point close to 1. The three-nucleon ($3N$) system is the simplest testing ground for our understanding of the NN interaction in the presence of additional nucleons. Here one can study the bound states of ^{3}H and ^{3}He, the elastic nucleon-deuteron (Nd) scattering or the Nd-breakup process. The Nd breakup, where three free nucleons appear in the final state, is particularly

* Dedicated to Prof. W. Glöckle on the occasion of his 60th birthday

interesting. It contains rich physical information since the nucleon momenta are not integrated over the deuteron wave function. Moreover, for the 3*N* system the observables can be calculated in a numerically exact way by using the Faddeev formalism with both 2*N* and 3*N* forces taken into account [1]. Therefore the *NN*-interaction can be tested reliably in the 3*N* system by a direct comparison of exact theoretical predictions with accurate experimental data.

Although some of the measured 3*N* observables are described well by modern realistic potentials, there are also discrepancies [1]. These discrepancies are particularly interesting as they could call for new ingredients in addition to 2*N* forces, namely for genuine 3*N* interactions. Establishing clear cases for such discrepancies requires a sufficiently rich set of accurate experimental data. The existing data set for the breakup process is much poorer than the one for elastic scattering. Most breakup experiments performed up to now were restricted to specific kinematical configurations like quasi-free scattering, collinearity or symmetric space star configurations (see ref. [1] and references therein). Results of these experiments suggest that in principle no 3*N* force is necessary – theoretical predictions based solely on the 2*N* force essentially agree with the data. However, there are notable disagreements in some configurations, especially in the symmetric space star configuration, measured at lower energies, where theoretical predictions overestimate *pd* data and underestimate *nd* data. The Coulomb interaction totally neglected in the calculation is probably the reason of the disagreement of the theory with the *pd* data. The reason of the disagreement with the *nd* data is unknown and this problem is still under investigation [2]. Also in the case of the elastic scattering there are discrepancies between modern 2*N*-potential predictions and the experimental data. A well-known case is the low-energy analyzing power A_y, where both *nd* and *pd* data in the region of the A_y maximum are clearly underestimated by theoretical predictions based on the modern 2*N* potentials [1, 3]. Present-day 3NF models introduce only very minor effects and do not remove these disagreements. One possible explanation of the problem is that in the recent phase-shift analysis the ^3P 2*N* phase-shift parameters, to which A_y is very sensitive, have not been set to their correct values [4]. If these discrepancies are not due to wrong 2*N* forces, a 3NF with still unknown properties may be a candidate for solving the problem. In ref. [5] arguments are given for such a scenario. Up to now, however, this A_y problem is still an unsolved puzzle. Another example of a significant discrepancy appears in the minima of the elastic-scattering cross sections at higher energies, above around 60 MeV. A large part of these discrepancies can be removed when the TM 3NF, properly adjusted to the triton binding energy, is included in the 3*N* Hamiltonian [6]. It is very probable that in certain regions of the phase space for the breakup process, where the 2*N*-force-only cross section is small, the effect of the 3*N* force can be decisive. Therefore experimental studies of less explored regions of the phase space are very important.

We report here the cross sections and vector-analyzing powers obtained in the kinematically complete measurement of the $^2\mathrm{H}(\boldsymbol{p}, pp)n$ reaction at an energy $E_p^{\mathrm{lab}} = 65\,\mathrm{MeV}$ in four unspecific configurations: $(\vartheta_1, \vartheta_2, \varphi_{12}) = (20.0^\circ, 20.0^\circ, 180.0^\circ)$, $(20.0^\circ, 45.0^\circ, 180.0^\circ)$, $(20.0^\circ, 75.6^\circ, 180.0^\circ)$, and $(20.0^\circ, 116.2^\circ, 0.0^\circ)$. The measured observables are compared to the theoretical predictions based on the exact solutions of the 3*N*-Faddeev equations, involving both 2*N* and 3*N* forces.

The next section presents a brief description of the experiment. The theoretical scheme is sketched in Sect. 3. The data are compared with the theoretical predictions using $2N$ and $2N + 3N$ forces in Sect. 4. A summary and conclusions are given in Sect. 5.

2 Experiment

The four unspecific configurations discussed in this paper were measured together with the already published ones [7]. For a detailed description of the experimental set-up as well as of the evaluation procedure we refer to refs. [7, 8]. Below, a brief description and modifications of the applied procedures are given.

2.1 Experimental Setup

The experiment was carried out at the Paul Scherrer Institute in Villigen, Switzerland. The transversally polarized proton beam with an energy of 65 MeV, a polarization of about 0.75 and an intensity of about 250 nA was focused on a deuterium gas target. To reduce systematic errors the beam polarization was reversed every second.

Protons and deuterons were detected by semiconductor surface-barrier detectors (SBD) at the largest (116.2°) angle and by plastic-scintillator $\Delta E - E$ telescopes at all remaining positions (Fig. 1). The detectors were arranged symmetrically on both sides of the beam axis to suppress systematic errors and to increase counting statistics. The use of $\Delta E - E$ telescopes and the measurement of the time-of-flight

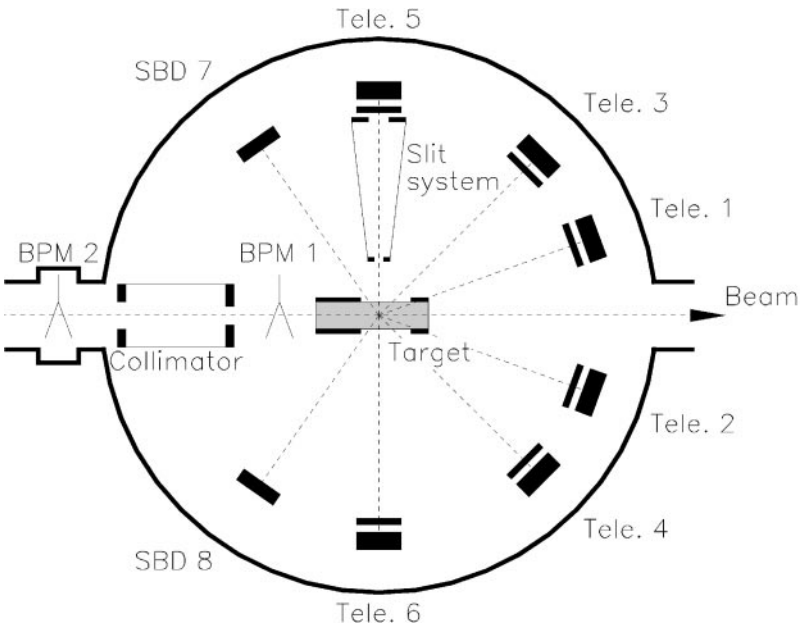

Fig. 1. Schematic view of the scattering chamber with detectors. Only one detector-slit system is shown as an example. Beam profile monitors (BPM1 and BPM2) and beam-collimator slits are also shown. All shielding materials are omitted. Relative dimensions of the elements are not to scale

difference between both coincident particles allowed us to distinguish protons from deuterons and to determine random coincidences.

All detectors were equipped with appropriately chosen slit systems defining the solid angles. The dimension of the beam-target crossing volume has been determined by monitoring the beam profiles (using BPM1 and BPM2) throughout the experiment.

An on-line data-acquisition system collected coincidences for each pair of detectors. Simultaneously, for the purpose of the cross-section normalization, single events with the rate reduced by a factor of 1000, to a level acceptable for the data-acquisition system, were also accumulated. The coincidence-gate width was about 30% larger than the time distance between the neighbouring beam bursts what allowed for simultaneous measurement of random coincidences. They were used in the off-line analysis to subtract background of accidental events.

2.2 Data Analysis

In order to determine the kinetic energies of the measured protons the energy-calibration procedure was performed. A mixture of deuterium and hydrogen gases has been used as a target during these energy-calibration measurements. A set of calibration points was established for each telescope and SBD detector by changing its angular position and identifying peaks corresponding to the well-defined energy values of the elastically scattered protons from the $^2\mathrm{H}(p,p)^2\mathrm{H}$ and $^1\mathrm{H}(p,p)^1\mathrm{H}$ processes.

To eliminate unwanted events the following procedure was used: The particle identification and the subtraction of ''pure'' random coincidences were handled as described in ref. [7]. The coincident events of protons originating in the breakup reaction form a narrow band around the three-body kinematical curve calculated for a ''point-like'' experimental geometry. This kinematical condition was used for a further reduction of background. The details are described in ref. [8]. Next, the events were projected onto the three-body kinematical curve. This projection resulted in one-dimensional spectra of coincidences as a function of the arc length S along the kinematics.

The breakup cross sections were determined by binning these spectra of coincidences along the arc length S. For the normalization we used the $p + {}^2\mathrm{H}$ elastic-scattering cross sections (measured by Shimizu et al. [9]), which were extracted in turn from the single spectra of elastic events measured simultaneously with the breakup ones. The appropriate construction of the slit systems, which defined the solid angles, guaranteed that the solid angle of the one telescope in each pair canceled in the ratio of the breakup to elastic-scattering cross sections. The differential cross section is then given by the following formula,

$$\frac{d^5\sigma_{\mathrm{br}}}{d\Omega_1\, d\Omega_2\, dS}(S,\Omega_1,\Omega_2) = \frac{d^2\sigma_{\mathrm{el}}}{d\Omega_1}(\Omega_1)\cdot\frac{N_{\mathrm{br}}(S,\Omega_1,\Omega_2)}{N_{\mathrm{el}}(\Omega_1)}\cdot\frac{1}{\Delta\Omega_2\,\Delta S}, \qquad (1)$$

where N_{br} is the number of breakup events projected into the arc-length bin, which is centered at S and ΔS-wide, $\Omega_i = (\vartheta_i, \varphi_i)$ are the polar and azimuthal angles of the i-th detector, $\Delta\Omega_i$ being its solid angle. $d\Omega$ is an abbreviation for $\sin\vartheta\, d\vartheta\, d\varphi$.

N_{el} is the number of particles scattered elastically into Ω_1. Events corresponding to different polarization states were summed up.

It was, however, not possible to use this method to normalize the data for the $(20.0^\circ, 20.0^\circ, 180.0^\circ)$ and $(20.0^\circ, 45.0^\circ, 180.0^\circ)$ configurations since the experiment has been optimized to measure configurations reported in ref. [7]. The solid angles relevant for coincident and single events ($\Delta\Omega_1^{coin}$, $\Delta\Omega_1^{sing}$, respectively) were slightly different and therefore the correction factor $\Delta\Omega_1^{sing}/\Delta\Omega_1^{coin}$ was calculated by integration over the whole active target volume with appropriate geometrical conditions. The reliability of this approach was tested for these configurations where a direct normalization was possible.

The discussion of experimental uncertainties is presented in all details in refs. [7, 8]. The systematic error of the cross-section normalization originating in the uncertainty of the geometrical width of the beam was found by changing this width within the range which was acceptable by other, directly normalized, configurations.

3 Theory

The theoretical results presented in this work are based on numerically exact solutions of the 3*N* Faddeev equations using realistic *NN* interactions. Taking into account only *NN* interactions and neglecting the long-range Coulomb force, the following Faddeev equations for the T operator are solved [1],

$$T = tP + tPG_0T, \tag{2}$$

where G_0 is the free three-body propagator, t is the two-body off-shell t matrix, and P is a sum of cyclical and anti-cyclical permutations of the three nucleons. After solving Eq. (2) the breakup transition operator U_0 can be calculated as

$$U_0 = (1 + P)T. \tag{3}$$

If the potential energy of the 3*N* system contains in addition to the pure two-body part also a term due to a three-nucleon force, V_4, then Eq. (2) changes its form to [10]

$$T = tP + (1 + tG_0)V_4^{(1)}(1 + P) + tPG_0T + (1 + tG_0)V_4^{(1)}(1 + P)G_0T. \tag{4}$$

The 3*N* force V_4 is split into three parts

$$V_4 = \sum_{i=1}^{3} V_4^{(i)}, \tag{5}$$

where each one is symmetrical under exchange of two nucleons. For instance, for the π-π-exchange 3*N* force [11] this corresponds to the three possible choices of the nucleon which undergoes the off-shell π-*N* scattering. Eqs. (2) and (4) are solved in a partial-wave-projected momentum-space basis. For more details we refer to refs. [1, 10] and references therein.

We have used the following charge-dependent *NN* interactions: Argonne v_{18} [12], CD Bonn [13], and Nijmegen I and II [14]. When solving Eq. (4) the 2π-exchange 3*N* Tucson-Melbourne force [11] was taken. The strong cut-off parameter Λ has been adjusted individually together with each *NN* force to the experimental triton binding [15]. In contrast to our previous studies (e.g., refs. [8, 16]) we

increased the number of 3*N* partial waves when including the 3*N* force. All 3*N* states with total angular momentum j in the two-nucleon subsystem up to $j \leq 3$ have been included.

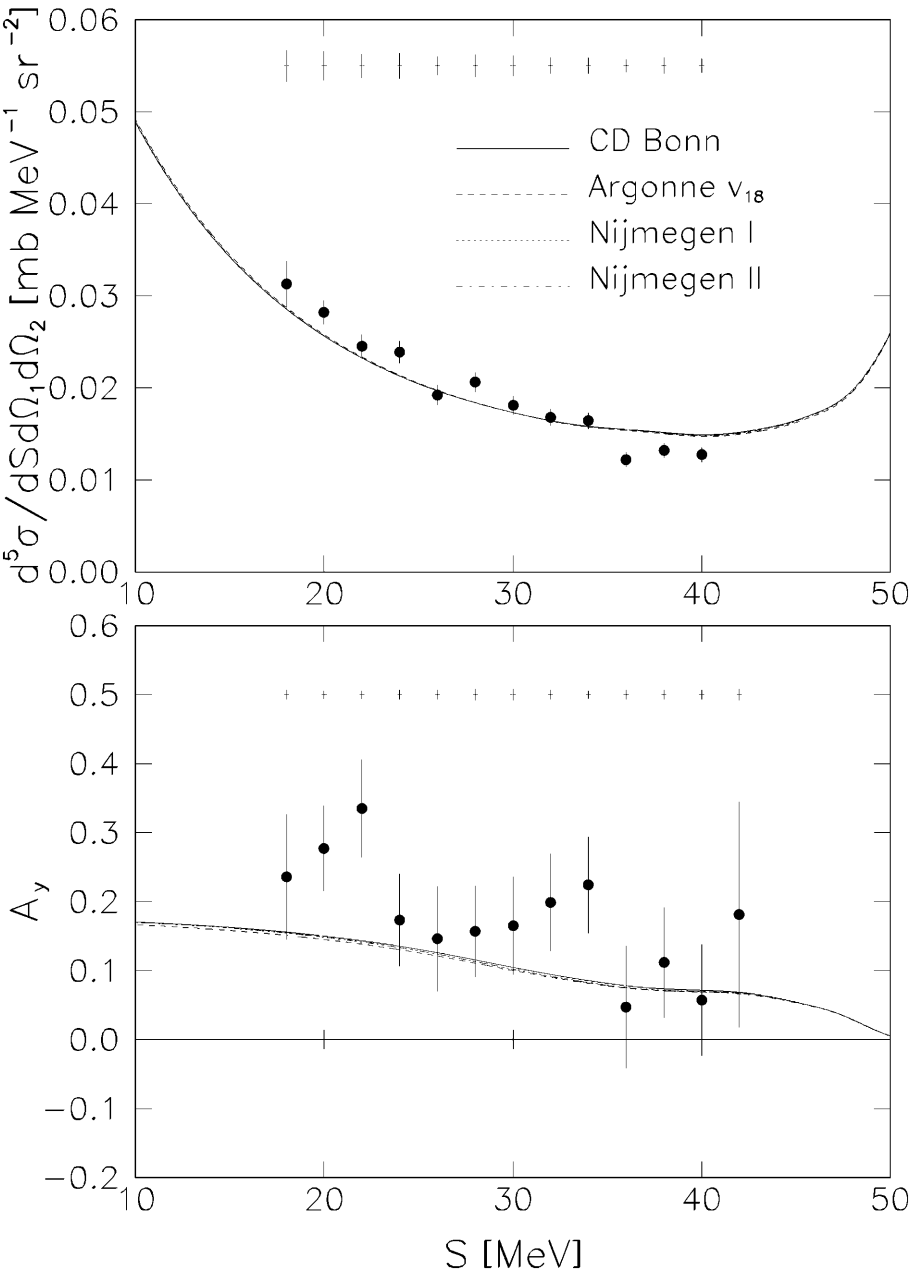

Fig. 2. Cross section and vector-analyzing power plotted as a function of the arc length of the kinematical curve for the $(20.0^\circ, 116.2^\circ, 0.0^\circ)$ configuration. Error bars attached to the experimental points represent the statistical uncertainties, whereas the systematic errors are shown above the distributions, separately for each point. The curves show the results of the Faddeev calculations using only 2*N* interactions. The theoretical predictions using Bonn CD (solid line), Argonne v_{18} (dashed), Nijmegen I (dotted), Nijmegen II (dash-dotted) almost coincide

4 Experimental Results and Comparison with Theory

Experimental results and theoretical calculations are presented as functions of the arc length S of the kinematical curve in Figs. 2–9. The experimental data are shown by full dots with the error bars representing the statistical uncertainty only. The systematic errors, also estimated individually for each data point, are shown separately above the dots.

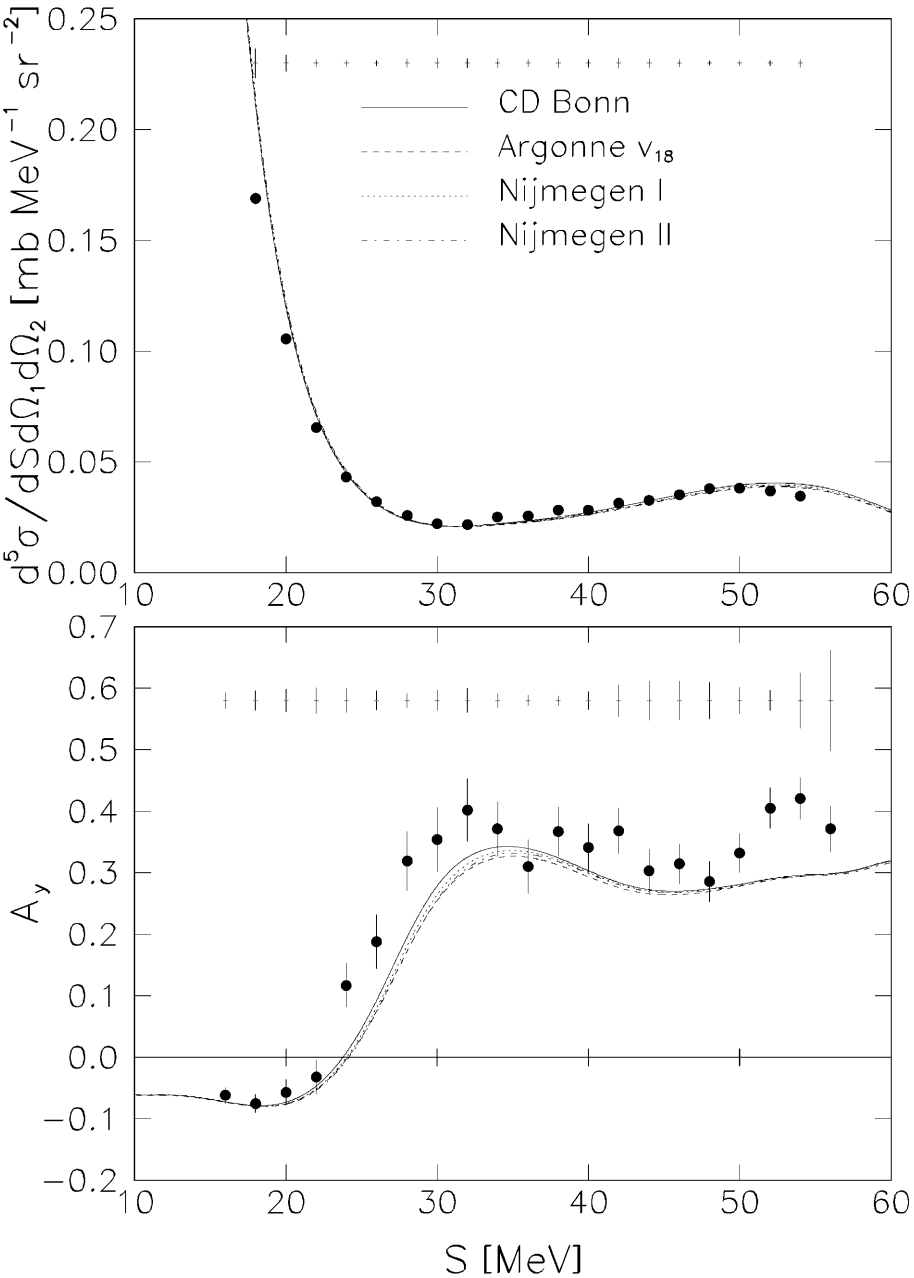

Fig. 3. Same as Fig. 2, but for the $(20.0°, 75.6°, 180.0°)$ configuration

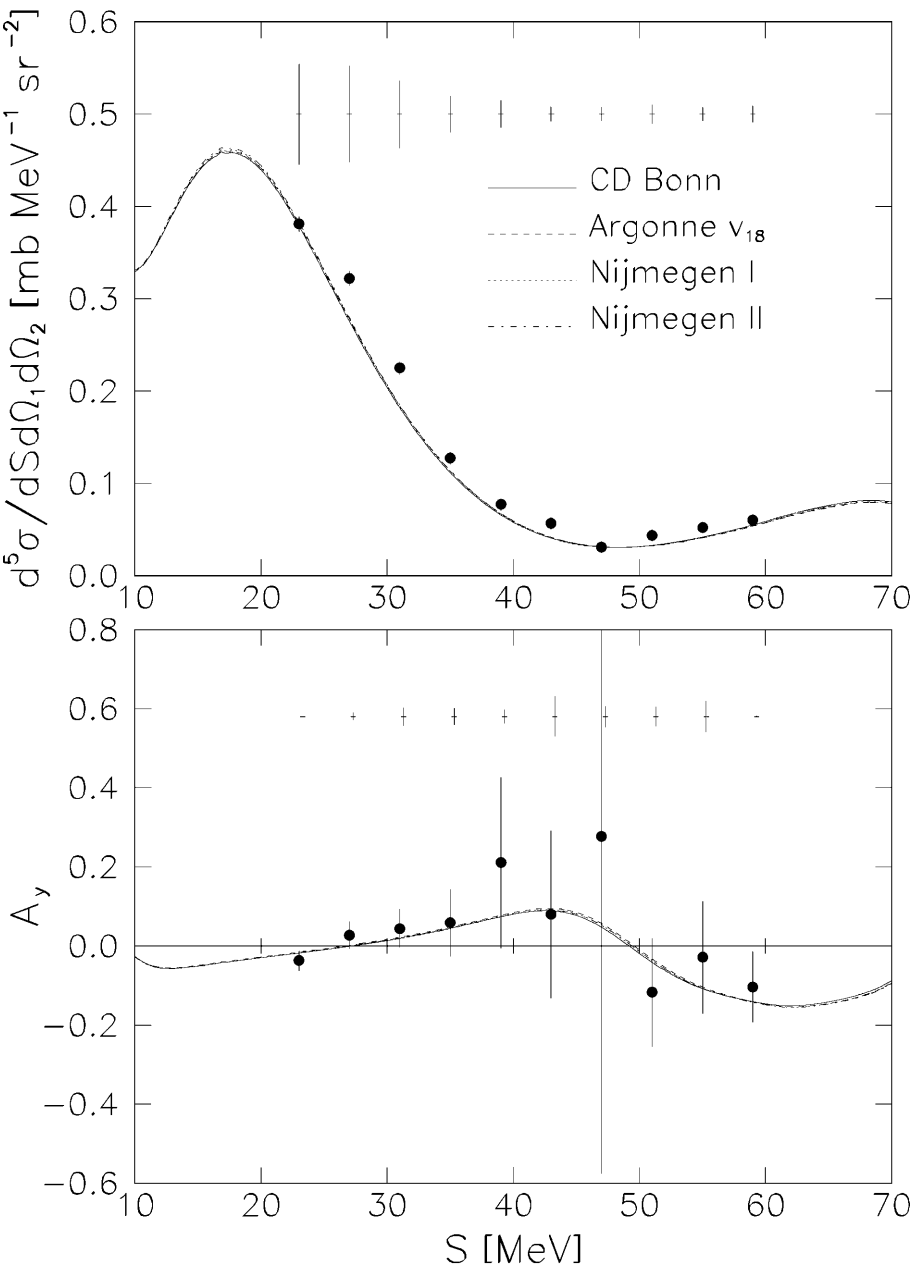

Fig. 4. Same as Fig. 2, but for the $(20.0°, 45.0°, 180.0°)$ configuration

All spectra obtained are presented even if large errors occur for some data points. As mentioned previously these large errors result from the fact that the experiment was optimized to measure other configurations. The systematic errors of the cross-section data are larger for the (20.0°, 20.0°, 180.0°) and (20.0°, 45.0°, 180.0°) configurations due to a less accurate normalization method. Larger level of accidental coincidences increased the statistical errors for the (20.0°, 116.2°, 0.0°) configuration. The (20.0°, 20.0°, 180.0°) configuration was measured by only one

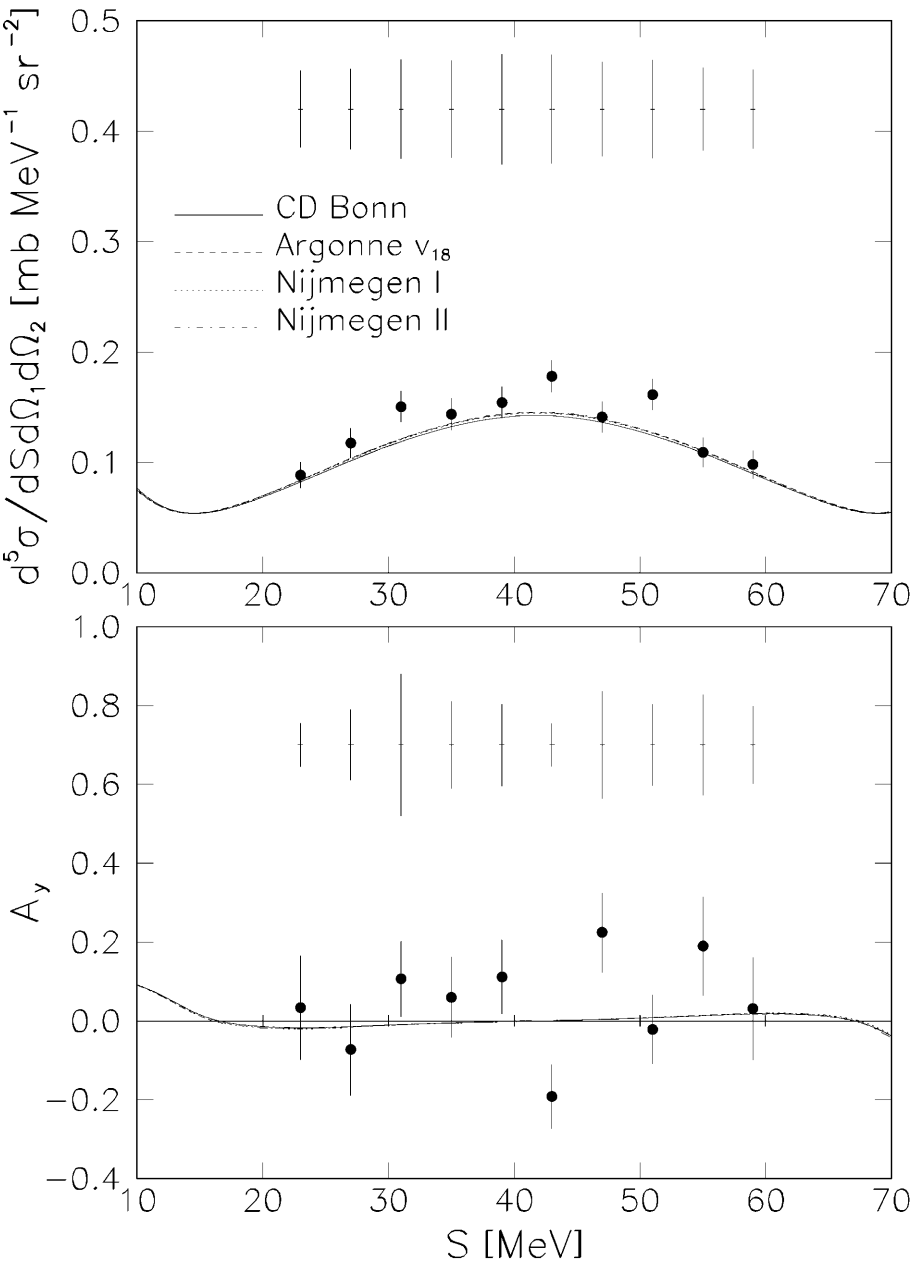

Fig. 5. Same as Fig. 2, but for the $(20.0^\circ, 20.0^\circ, 180.0^\circ)$ configuration

pair of detectors what increased both statistical and systematic errors. Nevertheless, also these three less accurately measured configurations are a useful test for checking theoretical predictions.

For all configurations studied the cross sections calculated with the CD Bonn, Argonne v_{18}, Nijmegen I, and Nijmegen II potentials are almost indistinguishable from each other and reproduce very well the experimental data (Figs. 2–5). Although the measurement of analyzing powers is more difficult one can notice that

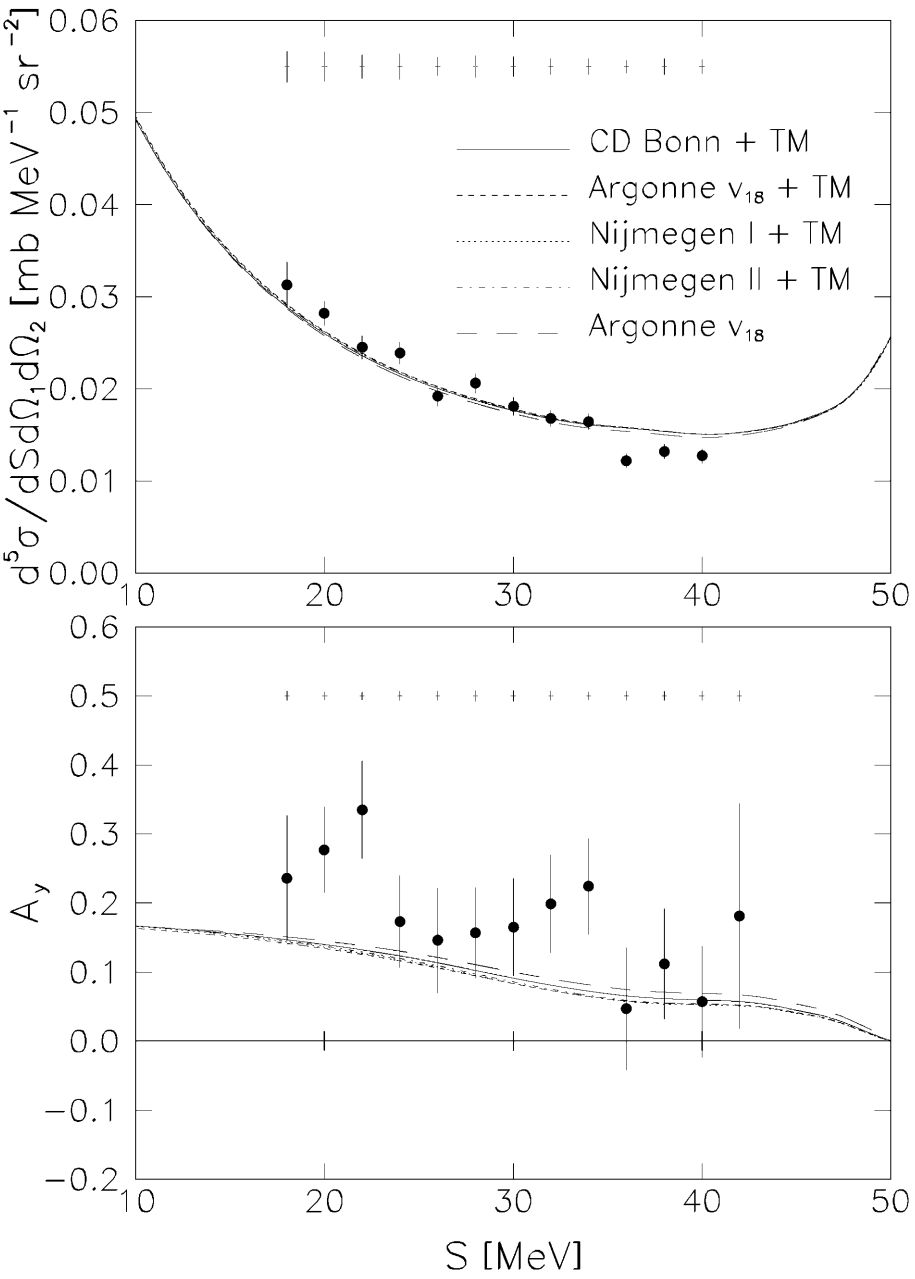

Fig. 6. Comparison of the experimental data with the calculations including the Tucson-Melbourne 3*N* force for the $(20.0°, 116.2°, 0.0°)$ configuration. The curves represent the results of the theoretical predictions including: Bonn CD + 3NF (solid line), Argonne v_{18} + 3NF (dashed), Nijmegen I + 3NF (dotted), Nijmegen II + 3NF (dash-dotted) and – as reference – pure 2*N* Argonne v_{18} (long-dashed)

the obtained A_y data agree well with the theoretical calculations, with exception of the (20.0°, 75.6°, 180.0°) configuration (the one, for which the results are most accurate), where some systematic discrepancies between theory and experiment are

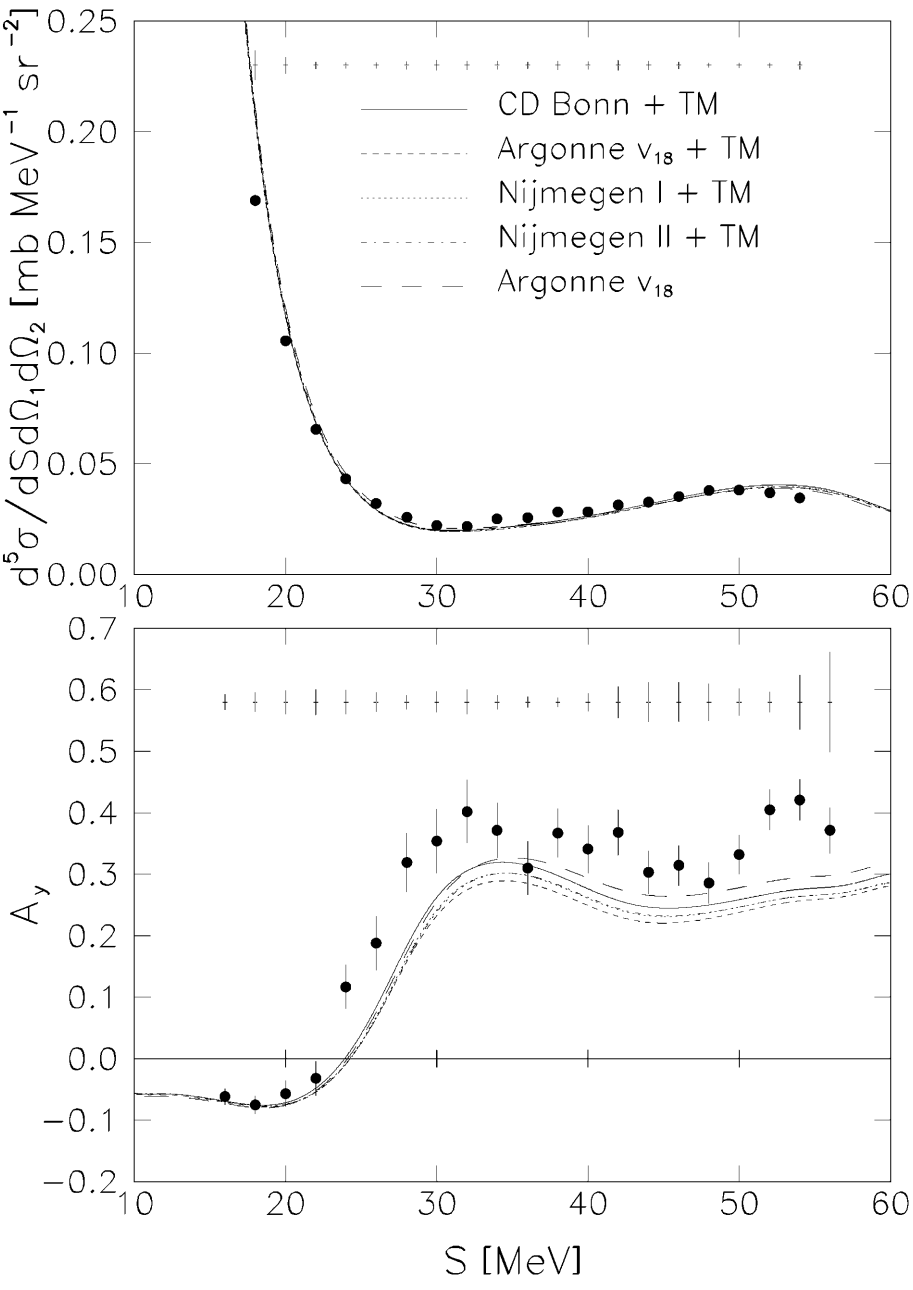

Fig. 7. Same as Fig. 6, but for the $(20.0^\circ, 75.6^\circ, 180.0^\circ)$ configuration

observed. In Figs. 6–9 the experimental data are compared with the calculations including the Tucson-Melbourne 3NF individually adjusted for each *NN* potential. For reference the calculations with pure 2*N* interaction (Argonne v_{18}) are also shown. For the cross sections the calculated 3NF effects are very small. They are somewhat larger for the analyzing powers. In the case of the $(20.0^\circ, 75.6^\circ, 180.0^\circ)$ configuration they seem to shift the theoretical predictions slightly from the experimental data.

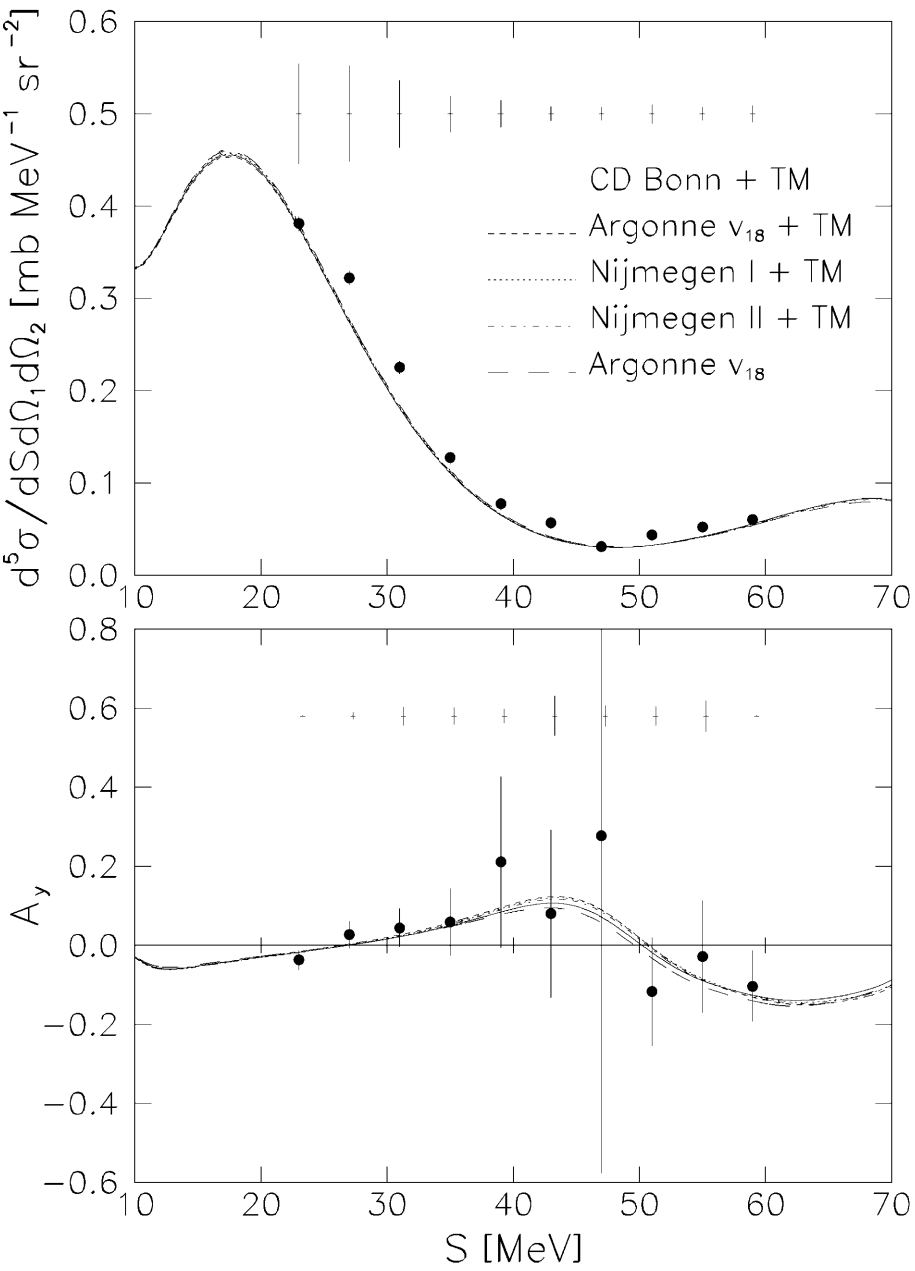

Fig. 8. Same as Fig. 6, but for the $(20.0°, 45.0°, 180.0°)$ configuration

5 Summary and Conclusions

Exclusive cross sections and vector-analyzing powers measured for the $^2\mathrm{H}(\boldsymbol{p}, pp)n$ reaction at $E_p = 65\,\mathrm{MeV}$ in four unspecific, arbitrarily chosen configurations have been compared to the predictions of modern, realistic *NN* potentials. For cross sections theory and experimental data agree very well with each other. A similar agreement is found for analyzing powers, with exception of the (20.0°, 75.6°,

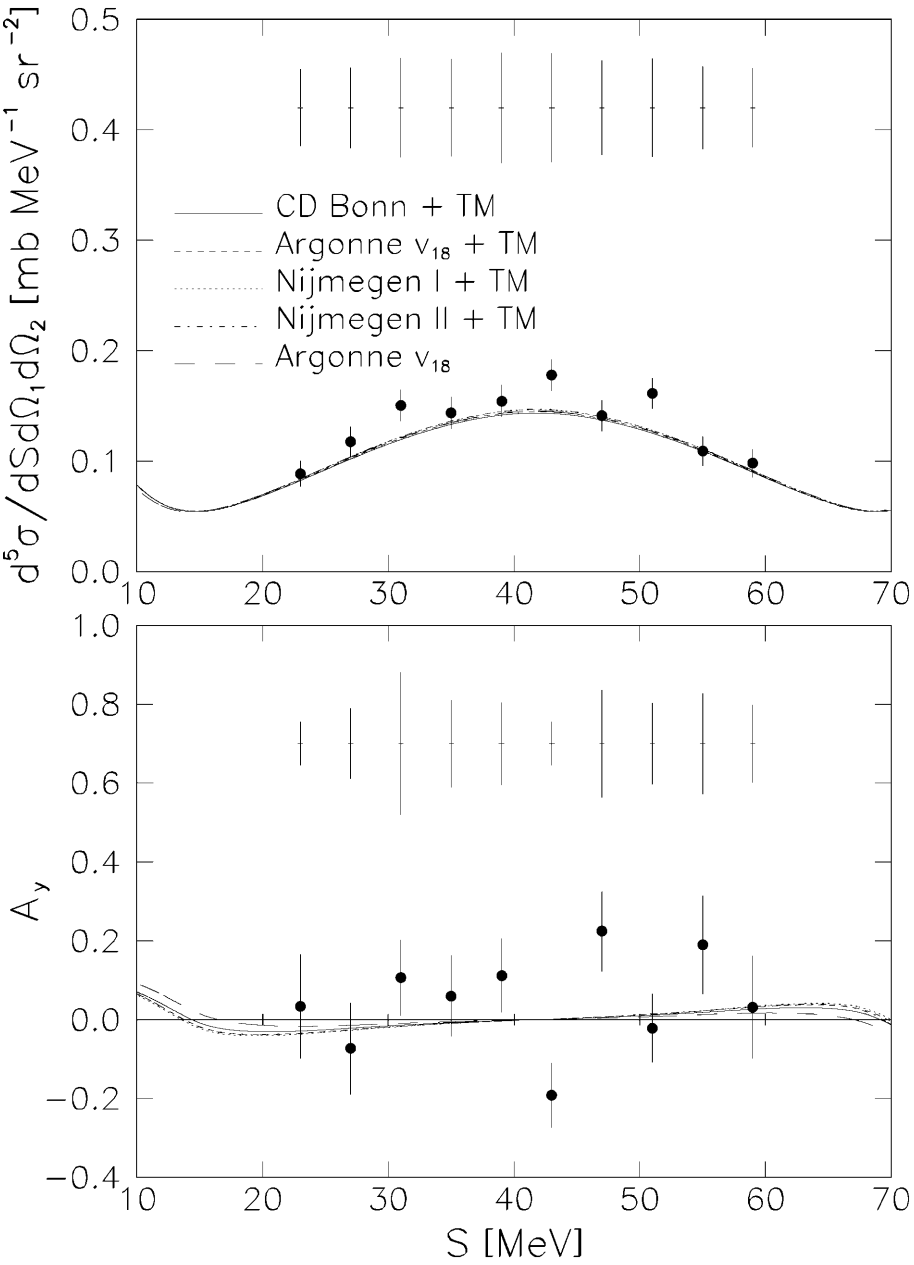

Fig. 9. Same as Fig. 6, but for the $(20.0°, 20.0°, 180.0°)$ configuration

$180.0°$) configuration, where pure $2N$-force predictions underestimate most of the data points. The inclusion of the Tucson-Melbourne 3NF, adjusted separately for every *NN* interaction to reproduce the triton binding energy, cannot explain the observed discrepancies. Moreover, the disagreement seems to be slightly increased. For other configurations the TM 3NF has practically negligible effects on both analyzing powers and cross sections. A similar behaviour of the TM 3NF has also been observed previously [8, 17] probably indicating its shortcomings and calling

for other 3NF constructions. On the other hand it ought to be stressed that the long-range Coulomb force between two protons is totally omitted in the present calculations. It might be supposed, however, that the effects of this neglect are not as large as the observed discrepancies at the rather high beam energy of the experiment discussed here. However, the final answer on the reason for the observed discrepancies between theory and data can be given only when calculations with exact treatment of the Coulomb force will be done.

It is interesting to note that there are no significant differences in the quality of the description of observables for the unspecific configurations discussed in the present paper and for the specific ones studied earlier [7, 8, 17], where some discrepancies for the vector-analyzing powers have also been found. Further investigations of the *pd*-breakup reaction, which will cover the available phase-space more systematically and will additionally deliver tensor-analyzing powers, will probably help to find other cases of discrepancies between experimental data and theory and will therefore form a valuable basis for testing future 3NF models.

Acknowledgement. This work was supported by the Polish Committee for Scientific Research under Grant No. 2P03B02818 and by the Swiss National Science Foundation. The numerical calculations were performed on the CRAY T90 and CRAY T3E of the Höchstleistungsrechenzentrum in Jülich, Germany, and on the CONVEX C3820 of the ACK-Cyfronet in Kraków, Poland (Grant No. KBN/UJ/054/95).

References

1. Glöckle, W., Witała, H., Hüber, D., Kamada, H., Golak, J.: Phys. Rep. **274**, 107 (1996)
2. Howell, C. R., Setze, H. R., Tornow, W., Glöckle, W., Hussein, A. H., Lambert, J. M., Mertens, G., Roper, C. D., Salinas, F., Šlaus, I., Gonzalez Trotter, D. E., Vlahowić, B., Walter, R. L., Witała, H.: Nucl. Phys. **A631**, 692c (1998)
3. Witała, H., Hüber, D., Glöckle, W.: Phys. Rev. **C49**, R14 (1994)
4. Tornow, W., Witała, H., Kievsky, A.: Phys. Rev. **C57**, 555 (1998)
5. Hüber, D., Friar, J. L.: Phys. Rev. **C58**, 674 (1998)
6. Witała, H., Glöckle, W., Hüber, D., Golak, J., Kamada, H.: Phys. Rev. Lett. **81**, 1183 (1998)
7. Allet, M., Bodek, K., Hajdas, W., Lang, J., Müller, R., Naviliat-Cuncic, O., Sromicki, J., Zejma, J., Jarczyk, L., Kistryn, St., Smyrski, J., Strzałkowski, A., Glöckle, W., Golak, J., Witała, H., Dechant, B., Krug, J., Schmelzbach, P. A.: Phys. Rev. **C50**, 602 (1994)
8. Zejma, J., Allet, M., Bodek, K., Lang, J., Müller, R., Navert, S., Naviliat-Cuncic, O., Sromicki, J., Stephan, E., Jarczyk, L., Kistryn, St., Smyrski, J., Strzałkowski, A., Glöckle, W., Golak, J., Hüber, D., Witała, H., Schmelzbach, P. A.: Phys. Rev. **C55**, 42 (1997)
9. Shimizu, H., Imai, K., Tamura, N., Nisimura, K., Hatanaka, K., Saito, T., Koike, Y., Taniguchi, Y.: Nucl. Phys. **A382**, 242 (1982)
10. Hüber, D., Kamada, H., Witała, H., Glöckle, W.: Acta Phys. Pol. **B28**, 1677 (1997)
11. Coon, S. A., Scadron, M. D., McNamee, P. C., Barret, B. R., Blat, D. W. E., McKellar, B. H. J.: Nucl. Phys. **A317**, 242 (1979); Coon, S. A., Glöckle, W.: Phys. Rev. **C23**, 1790 (1981)
12. Wiringa, R. B., Stoks, U. G. J., Schiavilla, R.: Phys. Rev. **C51**, 38 (1995)
13. Machleidt, R., Sammarruca, F., Song, Y.: Phys. Rev. **C53**, R1483 (1996)
14. Stoks, U. G. J., Klomp, R. A. M., Terheggen, C. P. F., de Swart, J. J.: Phys. Rev. **C49**, 2950 (1994)
15. Nogga, A., Hüber, D., Kamada, H., Glöckle, W.: Phys. Lett. **B409**, 19 (1997)

16. Bodek, K., Glöckle, W., Golak, J., Jarczyk, L., Kistryn, St., Kozłowska, B., Lang, J., Micherdzińska, A., Naviliat-Cuncic, O., Smyrski, J., Sokołowski, M., Sromicki, J., Strzałkowski, A., Witała, H., Zejma, J., Zipper, W.: Nucl. Phys. **A631**, 687c (1998)
17. Allet, M., Bodek, K., Golak, J., Glöckle, W., Hajdas, W., Hüber, D., Jarczyk, L., Kamada, H., Kistryn, St., Lang, J., Müller, R., Naviliat-Cuncic, O., Smyrski, J., Sromicki, J., Strzałkowski, A., Witała, H., Zejma, J.: Phys. Lett. **B376**, 255 (1996)

Received May 12, 1999; revised March 3, 2000; accepted for publication April 26, 2000